On the Effects of Different User Speeds on the Performance of High Speed Downlink Packet Access

Andreas Müller and Tao Chen
Nokia Research Center Beijing
People's Republic of China
And.Mueller@gmx.de, Tao.T.Chen@nokia.com

***Abstract*— In this paper, we analyze the impact of the velocity a mobile user is moving at on the performance of the high speed downlink packet access (HSDPA) in UMTS on both a qualitative and a quantitative level. In this context, we especially focus on the cell capacity as well as on the average per-user bit rates. As will be shown, the user speed has a significant influence on the system performance, which generally becomes worse with increasing velocities. We identify and classify the reasons for this performance degradation and examine their individual contributions as well as the overall performance decrease by means of extensive system level simulations. This contributes to a better understanding of the effects involved with higher user speeds and reveals where the biggest potential for performance optimizations can be found.**

I. Introduction

High Speed Downlink Packet Access (HSDPA) has been introduced in release 5 of the Universal Mobile Telecommunications System (UMTS) and can provide higher bit rates for packet data transmissions with peak data rates up to 10.8 Mbps. The key enabling technologies for reaching such high bit rates are *link adaptation* (LA) with *adaptive modulation and coding*, a fast *hybrid automatic repeat request* (HARQ) mechanism on the physical layer, a shortened *transmission time interval* (TTI) of 2 ms as well as fast scheduling algorithms in the Node-B, see for example [1], [2].

In the ideal case, the link adaptation in conjunction with an appropriate packet scheduler can follow the small-scale fading of the terminals, so that users are always scheduled when they observe rather good channel conditions and the corresponding data is transmitted using the *modulation and coding scheme* (MCS) with the highest spectral efficiency keeping the frame error probability below a certain threshold. For that purpose, all terminals usually send periodic channel quality feedback reports to the respective serving Node-B, containing a channel quality indicator (CQI) value, which is obtained from measurements of the common pilot channel (CPICH) and which indicates the modulation scheme, transport block size and the number of codes that currently might be used to transmit data to the corresponding user. However, as there is a certain delay between the measurement of the CPICH and the actual data transmission, the channel quality at the scheduling instant generally deviates from the reported channel quality. In order to compensate this bias, usually additionally an outer loop link adaptation mechanism based on the ACKs/NACKs from past transmissions is applied as proposed in [3], [4]. Such a mechanism can be realized by introducing a continuously adjusted CQI offset value, for instance, which is subtracted from all received CQI values in the Node-B before an appropriate MCS is selected. Thereby, it is possible to actively control the residual frame error rate after a certain number of HARQ transmission attempts.

The actual performance of HSDPA depends on many different factors, including the velocity the mobile users are moving at. In previous studies, performance aspects of HSDPA have primarily only been examined for a user speed of 3 kmph, corresponding to a slowly-walking pedestrian, for example. In [5], additionally the speed sensitivity of the HSDPA cell capacity for the ITU Pedestrian-A channel model has been examined for different transmit and receive antenna diversity modes and in [6] the round-robin and the proportional fair (P-FR) scheduler have been compared with respect to their performance for different user speeds. However, to the best of our knowledge, there is no existing comprehensive study focusing exclusively on the effects of different user speeds on the overall HSDPA system performance. In this paper, we give a comprehensive overview of these effects and we examine and quantify their individual impact on the HSDPA system performance by means of extensive system level simulations.

The remainder of this paper is structured as follows: In section II, we analyze the effects involved with higher user speeds in theory. Section III provides a brief overview of the used simulation model whereas the actual simulation results are presented in section IV. Finally, the conclusions are given in section V.

II. Effects Involved with Higher User Speeds

Basically, there are two major effects that can be observed at higher user speeds: On the one hand, the channel conditions change faster and become generally more unstable. On the other hand, the transition from one cell to another one becomes more likely, what results in higher handover-rates. Both effects are not HSDPA-specific, of course, but can rather be encountered in almost any cellular network. In the following, we go a little bit deeper into these two issues and we consider their concrete impact on the HSDPA system performance.

A. Faster-Changing Channel Conditions

Faster-changing channel conditions and especially an increased fading rate—as caused by higher user speeds—might lead to significant changes of the instantaneous channel conditions within one TTI, hence leading to a direct detector degradation. This is generally reflected by a higher frame error probability for a certain Es/No-value (energy per symbol over noise) and might lead to a considerable performance degradation of the high-speed downlink shared channel (HS-DSCH). At the same time, the frame error probability of the high-speed shared control channel (HS-SCCH) also increases, so that the probability of missing a data transfer on the HS-DSCH is getting higher. This, of course, also contributes to a worse performance compared to the low-speed case.

In addition, faster-changing channel conditions also have a negative impact on the HSDPA system performance due to the already mentioned delay between the sending of a CQI report and the actual data transmission on the HS-DSCH. The main reason for this is the fact that the CQI reports become more and more unreliable with increasing user speeds, because the current channel conditions at the actual scheduling instant might significantly deviate from the reported channel quality if the fading rate is relatively high. In case that a P-FR scheduler is used, this has a particularly bad effect, as this scheduler usually schedules users "on top of their fades" according to the *received* CQI reports. Consequently, the probability that the current channel conditions are (much) worse when the actual data transmission takes place is very high. For other scheduler types, such as the round-robin scheduler, the influence of this effect should be smaller, as in these cases the channel conditions at the actual scheduling instants are often even better than the reported channel quality.

For the P-FR scheduler, the aforementioned effect also implies that the users are not necessarily scheduled "on top of their fades" anymore if the real channel conditions at the actual scheduling instant are considered rather than the reported channel qualities. This results in some kind of scheduling error and consequently also contributes to a performance degradation at higher user speeds.

B. Higher Handover-Rates

Aside from the general effects involved with higher handover-rates, such as an increasing amount of signaling traffic—what we do not consider here—, there are some specific effects that can only be found for HSDPA. Basically, these effects only occur in case of inter-Node B handovers while the transfer from one cell to another one is almost uninterrupted in case of intra-Node B handovers, cf. also [1].

As the scheduling is done in the Node Bs, they have to buffer MAC-d PDUs delivered by the RNC before transmitting them to the actual terminals. If an inter-Node B handover occurs, all buffered PDUs are usually simply discarded, including all pending PDUs which have already been sent but not acknowledged yet. Assuming that there is no intelligent handover control and that RLC acknowledged mode is used, the RLC layer has to take care of this by initiating the retransmission of these PDUs to the new serving Node B. However, it takes some time to detect such a packet loss, what leads to higher delays and a certain inactivity period for the affected users. The time needed to detect a handover is mainly determined by the T1 timer of the MAC-hs layer, which specifies the maximum amount of time the MAC-hs layer waits before forwarding out-of-order PDUs to the MAC-d layer in order to avoid unnecessary RLC retransmissions. Immediately after a handover was performed, the RLC layer usually just continues to transfer PDUs to the new serving Node B, not being aware that some previous PDUs have been discarded. Upon reception of these out-of-order PDUs, the terminal first stores them in a buffer and only after expiration of the T1 timer, the first out-of-order PDU is forwarded to the MAC-d and RLC layer, whereupon finally a RLC NACK for each missing PDU is sent to the RNC. In order to reduce this delay, [7] specifies the possibility to trigger the sending of an RLC status report immediately after a handover was performed.

Furthermore, both the outer loop link adaptation as well as the commonly used P-FR scheduler always need some time to converge after a user has moved to a new cell. For that reason, the data transmission is usually relatively unreliable during the first transmission attempts, what results in higher frame error probabilities and possible scheduling errors. Normally, there is also an initial scheduling delay after a handover was performed, so that the associated dedicated channels have enough time to align their power. During this time, the affected users cannot be scheduled, what affects the average per-user bit rates as well as the multi-user diversity degree of the respective cell and thus to some extent also the overall cell throughput.

III. System Model and Configuration

For quantifying the impact of the effects involved with higher user speeds, we performed several system level simulations. The most important parameter settings are put together in table I. The basic principles of the used simulator are the same as presented in [8]. All simulations were performed for a macro cell scenario, consisting of a hexagonal grid comprising 18 cells, which are covered by identical 3-sector base stations with a site-to-site distance of 2.8 km. The used antennas have a 3 dB beam width of 65 degrees and do not support any transmit diversity mode. In order to avoid border effects, we made use of the wrap-around technique. The simulator operates at slot level and utilizes the actual value interface (AVI) for determining the frame error probability based on the mean signal-to-interference ratio measured over one TTI [9].

The total attenuation of the transmitted power is made up of the deterministic path loss according to the COST 231 Hata model, a log-normally distributed shadow-fading process with a standard deviation of 8 dB and 50 meters coherence distance, and a small-scale Rayleigh fading process according the Jakes model. We restrict to considering the ITU Vehicular-A power delay profile only, as this model is more realistic for scenarios where users are moving at relatively high speeds, such as highways, for example. The total simulation time was 300,000 slots, what corresponds to a duration of 200 seconds.

TABLE I

MOST IMPORTANT PARAMETER SETTINGS

Parameter	Value
General Parameters	
Simulation time	300 000 slots
Simulation scenario	Macro cell, 18 sectors
Avg. number of users per cell	10
Power delay profile	ITU Vehicular-A
Path loss model	COST 231 Hata
Rayleigh fading model	Jakes
Std. deviation of shadow fading	8 dB (log-normally dist.)
HSDPA-Related Parameters	
Number of allocated codes	5
Power allocated for the HS-DSCH	7 W
Power allocated for the HS-SCCH	0.5 W
Packet scheduler	Proportional Fair (P-FR)
Initial scheduling delay	10 TTIs
Method for retransmissions	Chase Combining (CC)
CQI reporting factor (k-factor)	2
Minimum inter-TTI interval	1 TTI
Max. num. of SAW channels	6
Max. num. of retransmissions	4
T1 timer	200 ms
Default CQI reporting delay	3 TTIs
Std. dev. of CQI meas. error	1.5 dB (log-normally dist.)

The implementation of the HSDPA-specific mechanisms follows the release 5 specifications of 3GPP. We allocated five codes and a fixed power of 7 W for the HS-DSCH in every cell. The scheduling was realized by a P-FR scheduler according to [6]. The reported CQI value is calculated as the arithmetic mean out of three slot-based measurements of the power received on the CPICH and afflicted with a log-normally distributed measurement error with a standard deviation of 1.5 dB. The minimum inter-TTI interval was chosen to be one, i. e. the terminals can receive data in every slot. For simplicity, we restrict to considering time-multiplexing of different users only, but the fundamental results should look similar if also code-multiplexing is taken into account.

The fast physical layer HARQ mechanism supports six stop and wait (SAW) channels per user and at most four retransmissions. In case of retransmissions, soft combining according to the Chase combining principle is used [10]. If not otherwise stated, the delay between sending a CQI report and the time it is available at the packet scheduler/link adaptation entity in the Node-B was assumed to be 3 TTIs. While the transmit power used for the HS-DSCH is constant, the power for the HS-SCCH follows the power of the associated dedicated channel (DCH) with a fixed offset and an additional outer loop power control similar to the standard outer loop power control for dedicated channels.

We were using a full buffer traffic model, i. e. there is always application layer data available for every user. The parameters used for the outer loop link adaptation mechanism were chosen such, that the residual frame error probability after the first HARQ retransmission attempt is approximately 1 %, i. e. almost 99 % of all MAC-hs PDUs can be successfully transmitted with at most two HARQ transmission attempts. The initial scheduling delay, which determines how long the scheduler has to wait before scheduling a user who has entered a new cell in order to allow the associated dedicated channel to align its power, was set to 10 TTIs.

IV. SIMULATION RESULTS

A. Cell Capacity

Table II shows among others the simulation results for the average cell capacities assuming the parameter settings according to table I. It can be seen that there is a significant performance degradation for a speed of 20 kmph compared to the 3 kmph reference case, but for even higher user speeds the further performance degradation is only relatively small. This is because for a speed of 20 kmph the channel variations are already so fast, that the link adaptation cannot track them anymore. Therefore, a further decrease in the cell capacity for user speeds beyond 20 kmph results only from direct detector degradations and higher numbers of handovers, but not from an increased link adaptation error.

At a first glance, it seems to be surprising that the cell capacity for a user speed of 50 kmph case is higher than the capacity of the 20 kmph case, because basically one would expect a steady performance decrease with increasing terminal velocities. However, this can be explained as follows: The distance between two deep fades of the Rayleigh fading is usually in the order of half the wavelength of the carrier frequency. This means the mean distance between the "top of a fade" and the next deep fade is in the order of $\lambda/4$. For the considered scenario, the carrier frequency is 2 GHz, what corresponds to a wavelength of about 15 cm or equivalently $\lambda/4 = 3.75$ cm. The distance covered by a terminal during the assumed CQI delay of 3 TTIs is 3.34 cm for a user speed of 20 kmph and 8.34 cm for a user speed of 50 kmph, what corresponds to $0.22\,\lambda$ and $0.56\,\lambda$ respectively. As the used P-FR scheduler schedules users always "on top of their fades" and due to the CQI reporting delay, the probability that a user moving at a speed of 20 kmph actually is in a deep fade at the actual scheduling instant is consequently very high whereas it is very likely that a user moving at a speed of 50 kmph is already on the top of the next fade at this instant. Therefore, the average link adaptation error is generally higher for the 20 kmph case compared to the 50 kmph, what is reflected by the

TABLE II

BASIC SIMULATION RESULTS

User Speed [kmph]	3	20	50	80
Cell Capacity [Mbps]	1.613	1.009	1.027	0.944
Relative Performance	100 %	62.6 %	63.7 %	58.5 %
Mean CQI Offset	2.67	4.66	4.22	3.41
Mean Avg. User Bit Rate [kbps]	161.8	101.4	103.7	96.3
Std. Dev. of Avg. User Bit Rate [kbps]	54.3	46.8	50.3	58.0
Coeff. of Variation	0.336	0.462	0.485	0.602

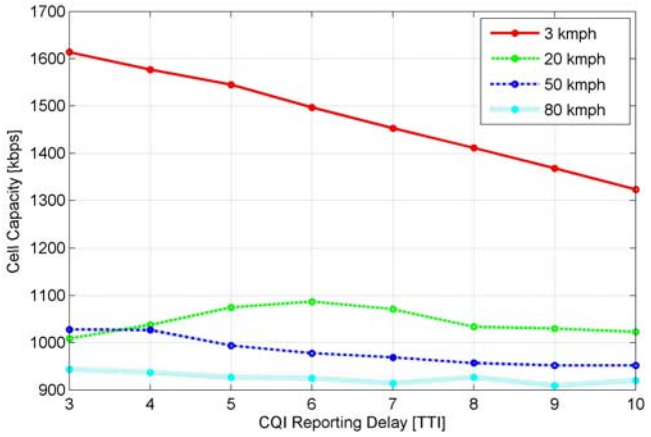

Fig. 1. Dependency of the Cell Capacity on the CQI Reporting Delay

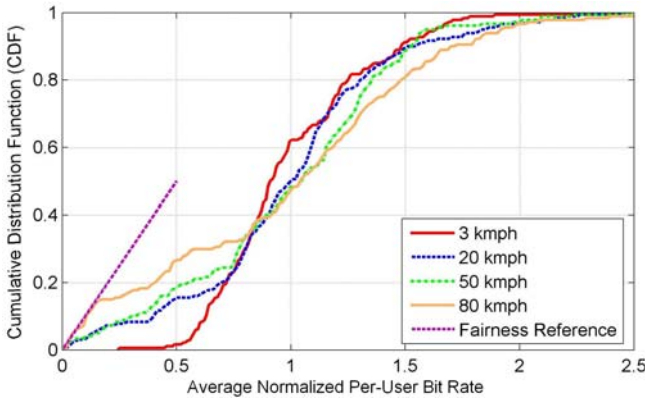

Fig. 2. Distribution of the Average Normalized Per-User Bit Rates

mean values of the CQI offset introduced by the outer loop link adaptation mechanism, which is also contained in table II, as this mechanism tries to compensate this bias by increasing the value of this offset.

In order to further investigate this phenomenon, we performed several simulations with CQI reporting delays varying between 3 and 10 TTIs. The simulation results are displayed in figure 1. It can be seen that for the 20 kmph case the cell capacity first increases with increasing CQI delays and reaches its maximum for a delay of 6 TTIs. For this delay, the cell capacity is almost 10 % higher than for a delay of 3 TTIs, because the distance covered by the user during 6 TTIs is in the order of half the wavelength, so that the probability that the user is "on top of the next fade" at the actual scheduling instant is relatively high. Consequently, for CQI delays larger than 6 TTIs, the capacity is decreasing again. For the 3 kmph case, the cell capacity is steadily decreasing, as the deviation between the channel quality reported to the Node B and the channel quality at the scheduling instant is steadily increasing. The effect appearing for a speed of 20 kmph cannot be observed for user speeds of 50 and 80 kmph in figure 1, because the time needed for covering a distance corresponding to one fourth of the wavelength, i. e. the distance from the "top of a fade" to the next deep fade, is in the order of 2.7 and 1.7 TTIs respectively, what is not shown in figure 1 as 3 TTIs are considered to be the minimum achievable delay.

B. Average User Bit Rates and Fairness Considerations

For calculating the average user bit rates, we divided the number of successfully transferred bits on the application layer during one session by the total duration of the session. The mean values, the standard deviations as well as the coefficients of variation are all given in table II. The mean values are directly related to the cell capacity, of course, and can basically be obtained by simply dividing the cell throughput by ten, what corresponds to the average number of users per cell.

Figure 2 shows the cumulative distribution functions (CDF) of the average user bit rates normalized to the respective mean values for user speeds of 3, 20, 50 and 80 kmph. In addition to the CDFs, also the fairness reference curve according to [11] is shown. A system is considered to be 'fair' if the CDF of the normalized average per-user throughput lies right of the fairness reference curve. Obviously, this is fulfilled for all user speeds, but it should be noted that the coefficient of variation is increasing with increasing user speeds. For higher velocities, especially the probability that some users have a very low average bit rate is significantly higher, so one could say that for these velocities the degree of fairness is smaller than for the 3 kmph reference case.

C. Contribution of the Individual Effects

We performed several simulations in order to quantify the impact of the individual effects mentioned in section II on the HSDPA system performance, concentrating on the influence of higher handover-rates, the direct detector degradation, and the increasing channel variability—particularly the higher shadow (large-scale) and Rayleigh (small-scale) fading rates leading to a larger link adaptation error.

For quantifying the share of the direct detector degradation, we were using the AVI tables corresponding to a user speed of 3 kmph for *all* terminal velocities and compared the results with the original results presented in table II. This is a valid approach since the effects of the direct detector degradation and the other factors influencing the HSDPA system performance are completely uncorrelated in the used simulator.

Differentiating between the effects caused by higher handover-rates and the effects caused by the generally larger link adaptation error at higher user speeds is more difficult. A first approach would be to update the fading always according to a speed of 3 kmph whereas the actual moving speed remains unchanged and vice versa, i. e. updating the fading according to different user speeds whereas the actual movement of the terminal corresponds to a speed of 3 kmph. However, this leads to some problems, as the fading—and especially the shadow fading—is highly correlated with the handover-rate: If the shadow-fading is updated according to a user speed larger than the actual moving speed, an increased ping-pong effect, i. e. frequent handovers forth from and back to one cell in a rather short period of time can be observed, what makes it very

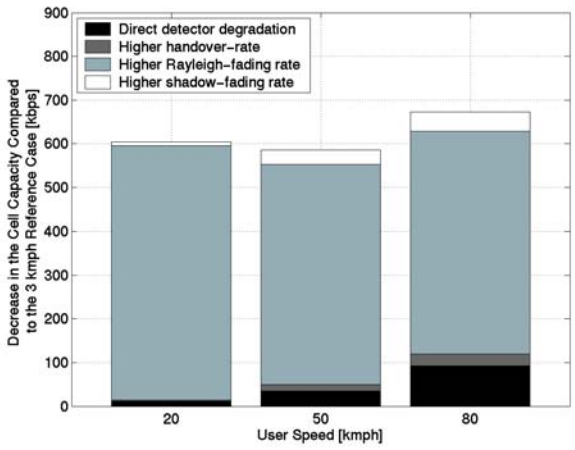

Fig. 3. Contribution of Different Effects to the Performance Degradation

difficult to clearly differentiate between the impact of higher handover-rates and higher fading rates. In order to overcome these problems, we performed several simulations as proposed in the previous paragraph, but switched the shadow fading completely off, as this is the main reason for the increasing ping-pong effect. This way, the aforementioned correlation basically does no longer exist and the individual effects can be clearly distinguished. The results obtained from these simulations were then compared with reference simulations according to the standard simulation setup, but also without considering shadow fading in order to get comparable results. By doing so, we could determine the relative share of the performance degradation caused by higher handover- and Rayleigh fading rates and extrapolate the absolute performance degradation due to these effects for the regular case with shadow fading by multiplying the respective relative shares with the absolute performance loss which can be extracted from table II. The residual share of the absolute performance degradation—which has not been caused by one of the other effects mentioned before—consequently stems mainly from the increased shadow fading rate.

The final results are presented in figure 3. It can be seen that the influence of higher handover-rates for fast-moving users are only marginal. This is primarily because the initial scheduling delay, the time needed to detect the discarding of buffered MAC-d PDUs in the Node Bs as well as the convergence time for the outer loop link adaptation and the P-FR scheduler are relatively small compared to the average sojourn of a user in one cell. However, this implies that results might look differently for other scenarios, such as micro or even pico cells. Depending on the actual user speed, the contribution of the direct detector degradation to the decrease of the cell capacity is in the order between 1 and 14 %. The apparently biggest share is caused by the higher Rayleigh (small-scale) fading rates whereas the effects of higher shadow fading rates are also relatively small.

V. Conclusions

In this paper, we have considered the effects involved with higher user speeds on the HSDPA system performance and we quantified them by presenting results obtained from extensive system level simulations. The two major effects that can be observed at higher user speeds are faster-changing channel conditions as well as higher handover-rates. As was shown, the performance of HSDPA in terms of the cell capacity is in the order of 40 % worse for user speeds of 20 kmph and beyond compared to the reference case with a user speed of 3 kmph. The biggest share of the performance degradation is caused by the fact that the link adaptation cannot track the faster-changing channel conditions anymore whereas the impact of the higher number of handovers is relatively small. However, for other environments than the considered macro cell scenario and especially smaller cell sizes, it might become more significant.

It was also shown, that the CQI reporting delay is a crucial factor of the performance and for some user speeds, a higher delay might improve the cell capacity due to the characteristics of the used P-FR scheduler, which always tries to schedule users “on top of their fades”. In addition, we have seen that the used P-FR scheduler remains fair for all considered user speeds, even though the variations of the average user bit rates are generally increasing with increasing terminal velocities.

Acknowledgment

The authors would like to thank Huibin Lin from Nokia Networks as well as Zhigang Yan and Jing Liu from China Mobile for their valuable comments and their support.

References

[1] “High speed downlink packet access (HSDPA): Overall description; stage 2,” 3GPP Technical Specification 25.308, version 5.6.0, Sept. 2004.
[2] H. Holma and A. Toskala, Eds., *WCDMA for UMTS*, 2nd ed. John Wiley and Sons, 2002.
[3] D. W. Paranchych and M. Yavuz, “A method for outer loop rate control in high data rate wireless networks,” in *Proceedings of the IEEE Conference on Vehicular Technology*, Sept. 2002.
[4] M. Nakamura, Y. Awad, and S. Vadgama, “Adaptive control of link adaptation for high speed downlink packet access (HSDPA) in W-CDMA,” in *Proceedings of the International Symposium on Wireless Personal Multimedia Communications (WPMC)*, Oct. 2002.
[5] J. Ramiro-Moreno, K. I. Pedersen, and P. E. Mogensen, “Network performance of transmit and receive antenna diversity in HSDPA under different packet scheduling strategies,” in *Proceedings of the IEEE Conference on Vehicular Technology*, Apr. 2003.
[6] T. E. Kolding, “Link and system performance aspects of proportional fair scheduling in WCDMA/HSDPA,” in *Proceedings of the IEEE Conference on Vehicular Technology*, Oct. 2003.
[7] “Radio link control (RLC) protocol specification,” 3GPP Technical Specification 25.322, version 5.8.0, June 2004.
[8] S. Hämäläinen, H. Holma, and K. Sipilä, “Advanced WCDMA radio network simulator,” in *Proceedings of the IEEE International Symposium on Personal, Indoor and Mobile Radio Conference (PIMRC)*, Sept. 1999.
[9] S. Hämäläinen, P. Slanina, M. Hartman, A. Lappeteläinen, H. Holma, and O. Salonaho, “A novel interface between link and system level simulations,” in *Proceedings of the ACTS Mobile Communications Summit*, Oct. 1997.
[10] F. Frederiksen and T. E. Kolding, “Performance and modeling of WCDMA/HSDPA transmission/H-ARQ schemes,” in *Proceedings of the IEEE Conference on Vehicular Technology*, Sept. 2002.
[11] “1xEV-DV evaluation methodology (V10),” 3GPP2 Technical Specification TSG-C.R1002, 2003.